

Resource-explicit interactions in spatial population models

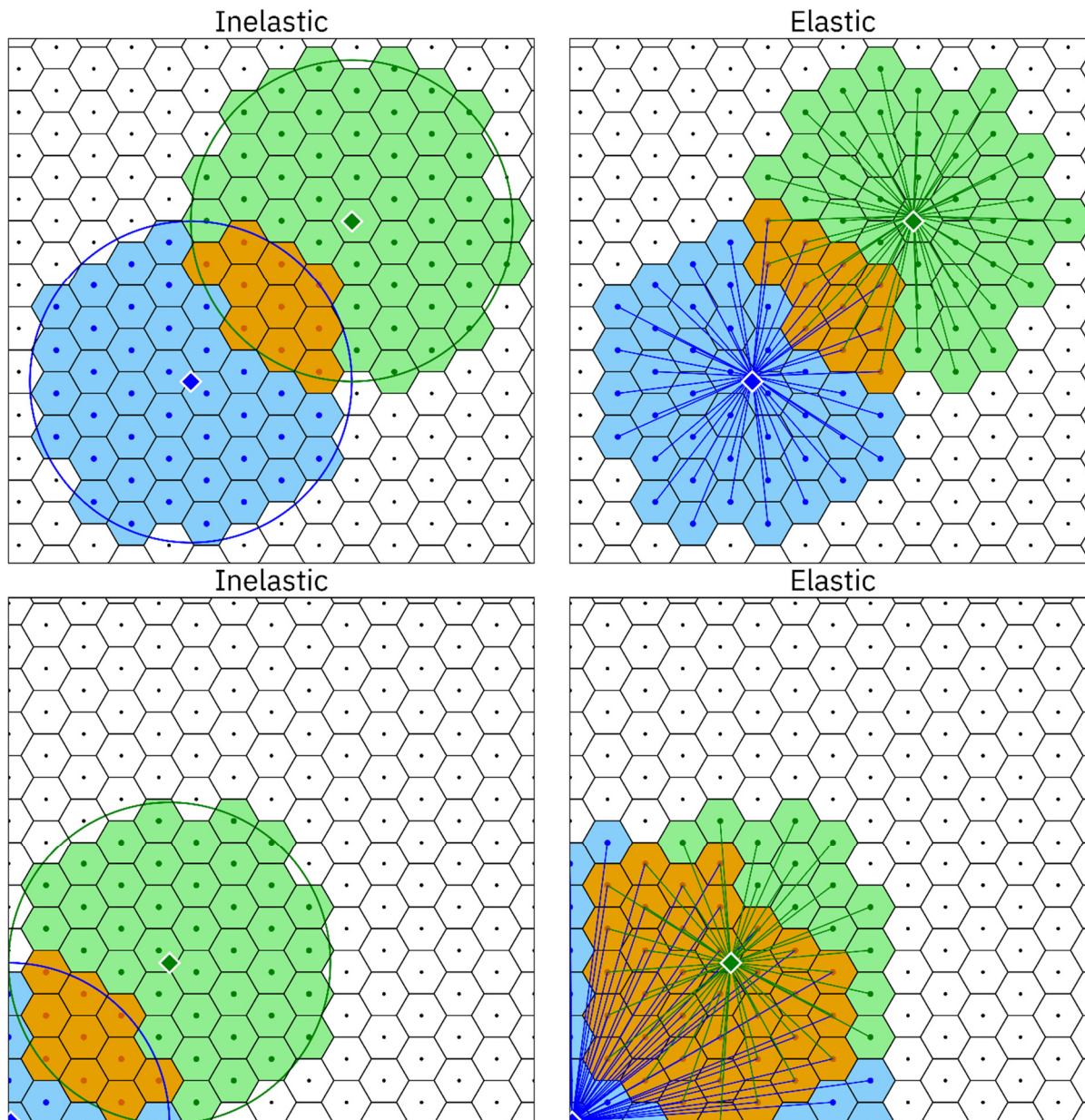
Supporting Information

1 RESOURCE NODE PLACEMENT METHODS

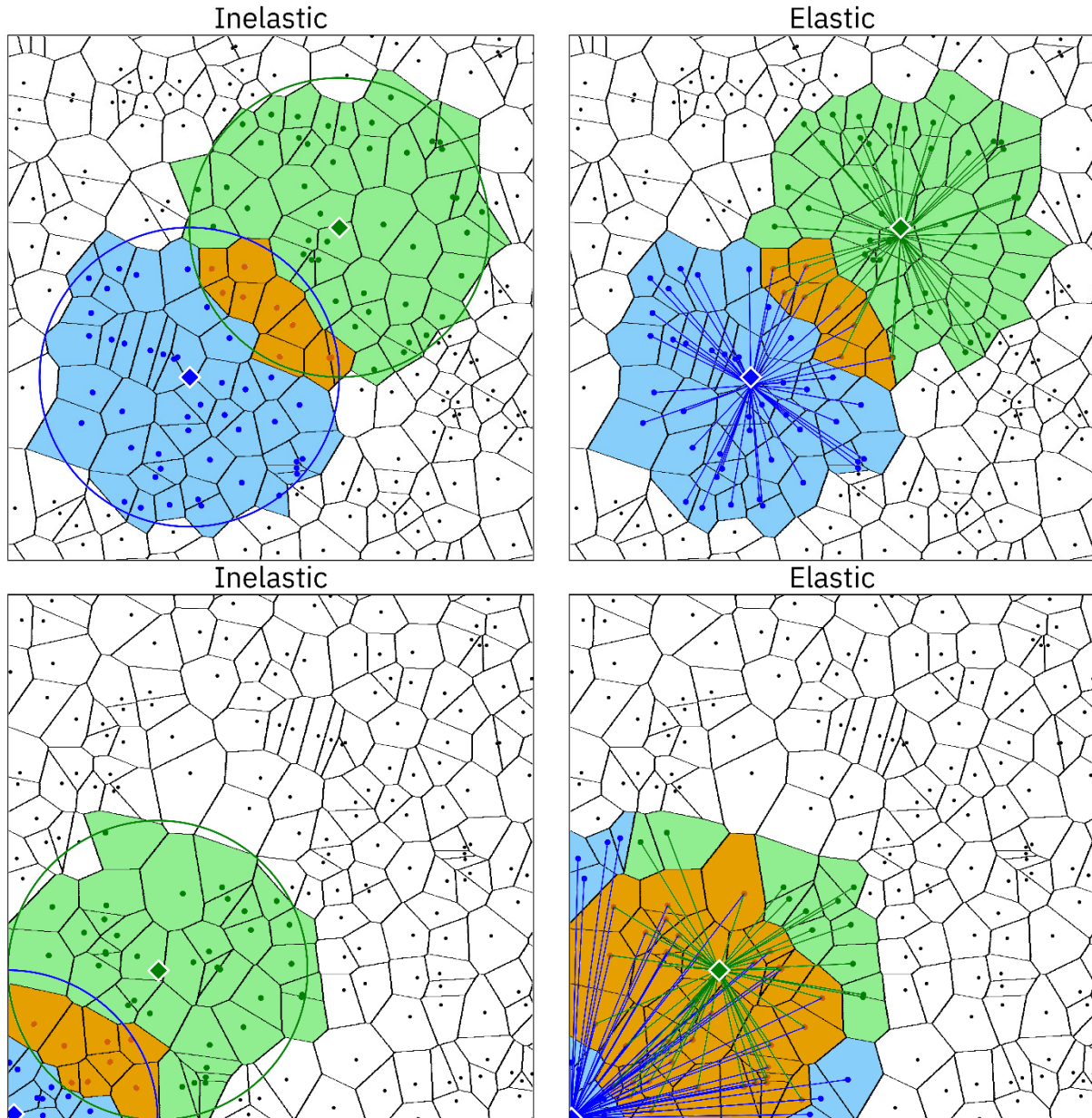
2 Three resource node placement methods were used in the models assessed
3 in this manuscript. These methods were: placing resource nodes at the center of
4 each square in a uniform square tiling of the landscape (Fig. 2), placing resource
5 nodes at the center of each hexagon in a uniform hexagonal tiling of the landscape
6 (Supplemental Fig. 1), and placing the resource nodes randomly across the
7 landscape, re-randomizing the placement of the nodes during each tick of the
8 model (Supplemental Fig. 2). Specifically, random placement was accomplished by
9 assigning each node an x and y coordinate randomly drawn from a uniform
10 distribution with a minimum of 0 and a maximum of the side length of the model.
11 For each of these placement methods, several resource node densities were tested.

12 In terms of code complexity, the randomized placement method is the
13 simplest. This method allows resource nodes to be added to the model with just a
14 few lines of code. The code to perform square and hexagonal tilings in our models
15 is significantly more complex due to the desire for the tiling to cover any square
16 area of arbitrary dimensions. To accomplish this, the grid of nodes is centered

17 within the modeled area, and nodes with areas that fall partially outside the
18 landscape are parameterized with a proportionately decreased amount of
19 resources. For example, if tiling a 2.8 by 2.8 landscape with square nodes that are
20 each 1 by 1, a 3 by 3 grid of nodes would be used, with the grid of nodes centered
21 within the area, and with nodes along the edges of the area are parameterized with
22 an appropriately reduced amount of resources given the portion of the node's area
23 that falls within the modeled area. In the hexagonally tiled models, the code
24 required to accomplish this task is somewhat more complex than in the square-
25 tiled models. That said, this complexity was included in the interest of matching
26 the direct-interaction models in this manuscript as closely as possible. In models
27 designed from the ground up as resource-explicit that do not need to match a prior
28 model, the landscape could be defined as having a boundary exactly matching a
29 desired grid of nodes, removing the need for this complexity. Minor adjustment to
30 these methods would also be appropriate if modeling a periodic area (such as a
31 toroidal landscape), in order to ensure appropriate resource availability along the
32 "seams" of the model.



Supplemental Figure 1. Visualization of resource-explicit interaction algorithms, hexagonal tiling. Competition between two individuals (blue and green diamonds with white outlines) is determined by the portion of their foraging area that overlaps and by the interaction algorithm used in the model. The foraging areas are represented by blue and green shading; the overlapping area is shaded orange. In the inelastic model (left), individuals forage from resource nodes (dots at the center of each hexagon) within their foraging radius. In the elastic model (right), individuals forage from as many nodes as necessary to maintain a nominally sized foraging area (in this case, that area comprises 50 nodes). In upper left panel, the blue individual happens to forage from only 49 nodes, and competition between these two individuals is slightly reduced. In the corner of the landscape, the difference between the two models is much greater: the blue individual has a much smaller foraging area in the inelastic model, while the blue individual in the elastic model forages from much further away to maintain a full-sized foraging area, resulting in greater competition.



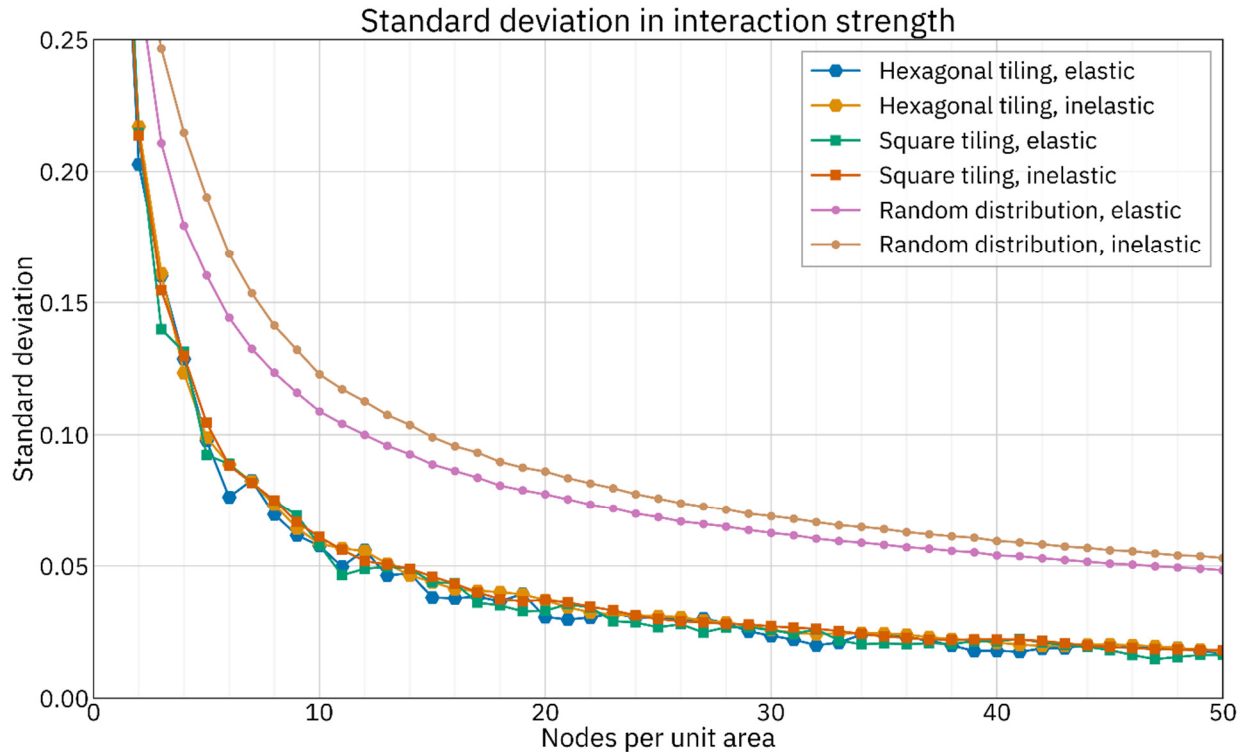
Supplemental Figure 2. Visualization of resource-explicit interaction algorithms, random node placement. Competition between two individuals (blue and green diamonds with white outlines) is determined by the portion of their foraging area that overlaps and by the interaction algorithm used in the model. The foraging areas are represented by blue and green shading; the overlapping area is shaded orange. In the inelastic model (left), individuals forage from resource nodes (dots at the center of each polygon) within their foraging radius. In the elastic model (right), individuals forage from as many nodes as necessary to maintain a nominally sized foraging area (in this case, that area comprises 50 nodes). When nodes are randomly distributed, the difference between the inelastic and elastic method even in the interior areas is greater. For example, the blue individual in the upper left panel forages from 53 nodes, and the green individual in the bottom left panel forages from 60 nodes, whereas in the elastic model, all individuals forage from 50 nodes, regardless of their position.

33 **Choice of node density and placement method.** As demonstrated in the Results
34 section, the choice of resource node density effects the runtime of the model as
35 well as the magnitude of variance in interaction strengths within the model. An
36 increased node density tends to yield a tighter distribution of interaction
37 strengths, but runs more slowly. The choice of node density must therefore be
38 made based on what kind of interaction strength variance can be can be
39 considered acceptable and how fast the model needs to run.

40 The choice between a regularly tiled model or a model with randomly
41 distributed nodes is also fairly straightforward. Models with regular tilings have
42 tighter distributions of interaction strengths, and run slightly faster compared to
43 models where the node positions are re-randomized during each tick of the model.
44 However, a model with randomized resource positions that are not re-randomized
45 could be used to represent a random heterogeneous landscape that is uniquely
46 generated each time the model is run. Random node placement could also be
47 combined with a landscape map to allow for the simulation of a specified
48 heterogeneous landscape without any pre-calculation step. Additionally, more
49 complex node placement strategies may provide desirable ways to represent
50 realistic resource variability. For example, nodes might be placed according to a
51 Poisson-Disc Sampling, in which entities are randomly placed, but are not placed
52 closer to one another than a specified minimum distance.

53 When minimizing variance in interaction strength is a priority, a regular
54 tiling of resource nodes is the best option (Supplemental Fig. 3; compare Figs 3
55 and 4 versus Fig. 5). This holds true both for simulations that are intended to
56 emulate a homogenous space (as is common in direct-interaction models) and for
57 simulations involving heterogeneous landscape maps (in which case pre-
58 calculating the appropriate amount of resources at each node and using a dense
59 tiling will result in the resource-explicit model matching the landscape as closely
60 as possible).

61 The choice between a hexagonal grid and a square grid is less consequential.
62 The two are almost interchangeable. Since a square grid is simpler to implement, it
63 may be the right choice for most models. In most cases, the standard deviation in
64 interaction strengths as compared to the circle-intersection function with one
65 tiling or another at a given density varies by no more than a percent or two
66 (Supplemental Fig. 3).



Supplemental Figure 3. Standard deviation of the differences in interaction strength between resource-explicit models and the circle-intersection function, square tiling. Two million pairwise interaction strengths measured by the circle-intersection function were subtracted from those measured in the resource-explicit models to yield a distribution for each model. The standard deviation was then measured for that distribution. This was repeated with tiling density ranging from 1 to 50 nodes per unit area. Note: while perhaps surprising, the cases where a denser tiling has a higher standard deviation are not due to measurement error (e.g., a hexagonally tiled elastic model with 7 nodes per unit area has a higher standard deviation than the same model with a density of 6 nodes per unit area).

67 There are only three possible ways to tile a plane with edge-to-edge
68 congruent regular polygons: using equilateral triangles, squares, or hexagons
69 (Birch et al., 2007; Grünbaum & Shephard, 1977). In other ecological modeling
70 contexts, such as modeling an area by using an array of panmictic demes linked by
71 migration, it is well accepted that spatial artifacts are smaller when using
72 hexagonal grids compared to using square grids (Birch et al., 2007). Without going
73 into complete detail, the reason the tiling does not matter as much in the resource-

74 explicit method is as follows: in our method, the *area* of each shape (be it a hexagon
75 or square) is determined by node density parameter. In linked panmictic models,
76 the *distance* between nodes is fixed by the model (with the distance between what
77 are considered to be different populations being related to the dispersal
78 characteristics of the species being modeled). Given a fixed distance between
79 nodes, a hexagonal tiling is a denser packing, with each hexagon therefore having
80 a smaller area than squares would have in a square tiling with the same distance
81 between nodes. Thus, a hexagonal tiling offers a large advantage in linked
82 panmictic models, but is not that different from a square tiling in our resource-
83 explicit models. However, in some cases, a hexagonal tiling has some desirable
84 properties in terms of minimizing unequal availability of resource nodes in the
85 inelastic model (see Supplemental Figs 14-19).

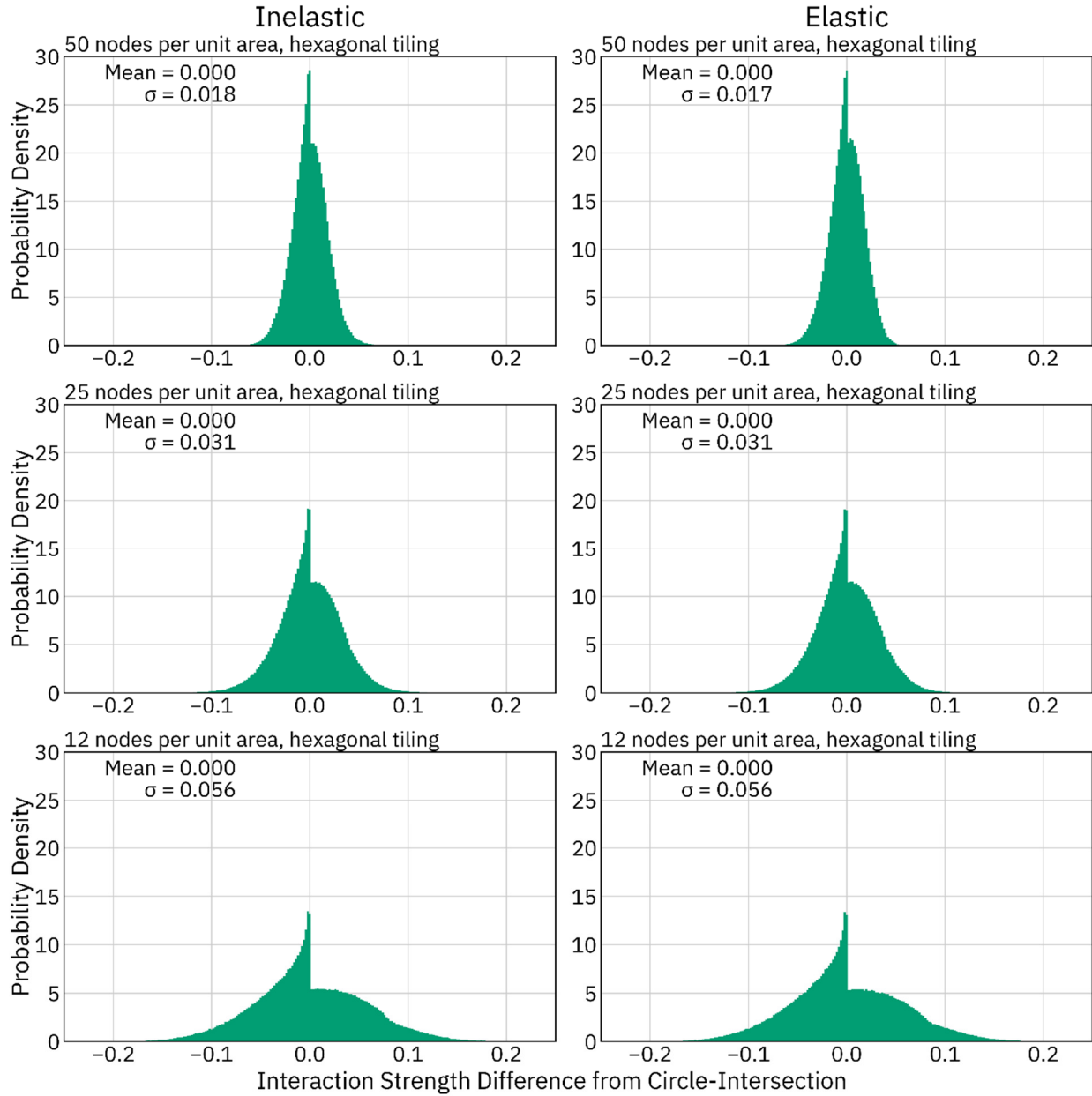
86 **DYNAMICS OF THE RESOURCE-EXPLICIT MODELS**

87 In the Results section, interaction strengths in the resource-explicit models
88 were assessed by measuring pairwise interactions between randomly placed
89 individuals. The interaction strengths measured in the resource-explicit models
90 were then subtracted from the strengths measured by the circle-intersection
91 function. This analysis was performed using a square tiling of the landscape (Fig.
92 4), a hexagonal tiling of the landscape (Supplemental Fig. 4), and with resource

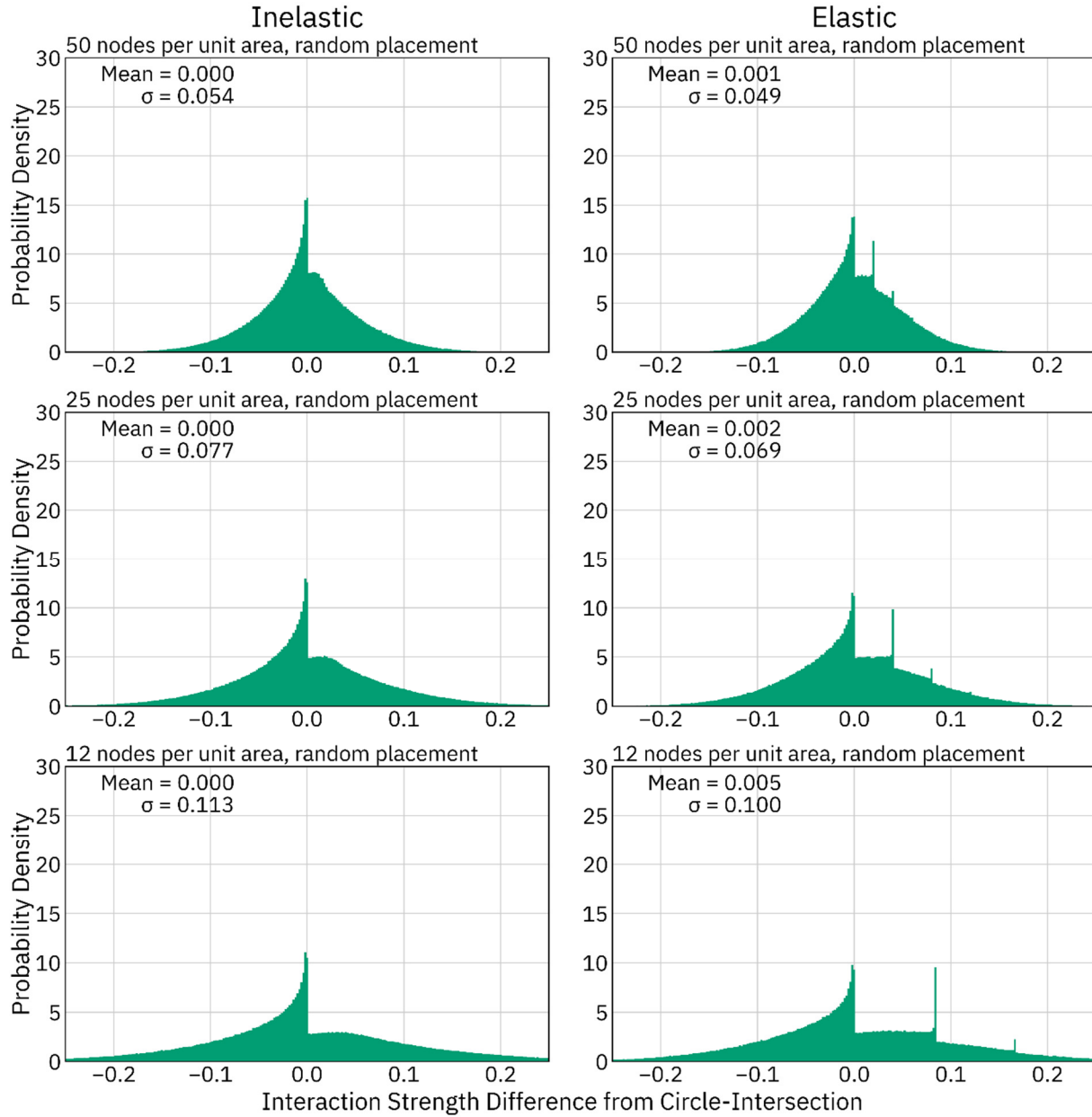
93 nodes randomly placed, with new positions drawn for each interaction measured
94 (Supplemental Fig. 5).

95 A further analysis was performed that compared the overall interaction
96 forces experienced by individuals in the resource-explicit models to that
97 calculated by the circle-intersection function. This analysis was performed using a
98 square tiling of the landscape (Fig. 5), a hexagonal tiling of the landscape
99 (Supplemental Fig. 6), and with resource nodes randomly placed, with new
100 positions drawn for each interaction measured (Supplemental Fig. 7).

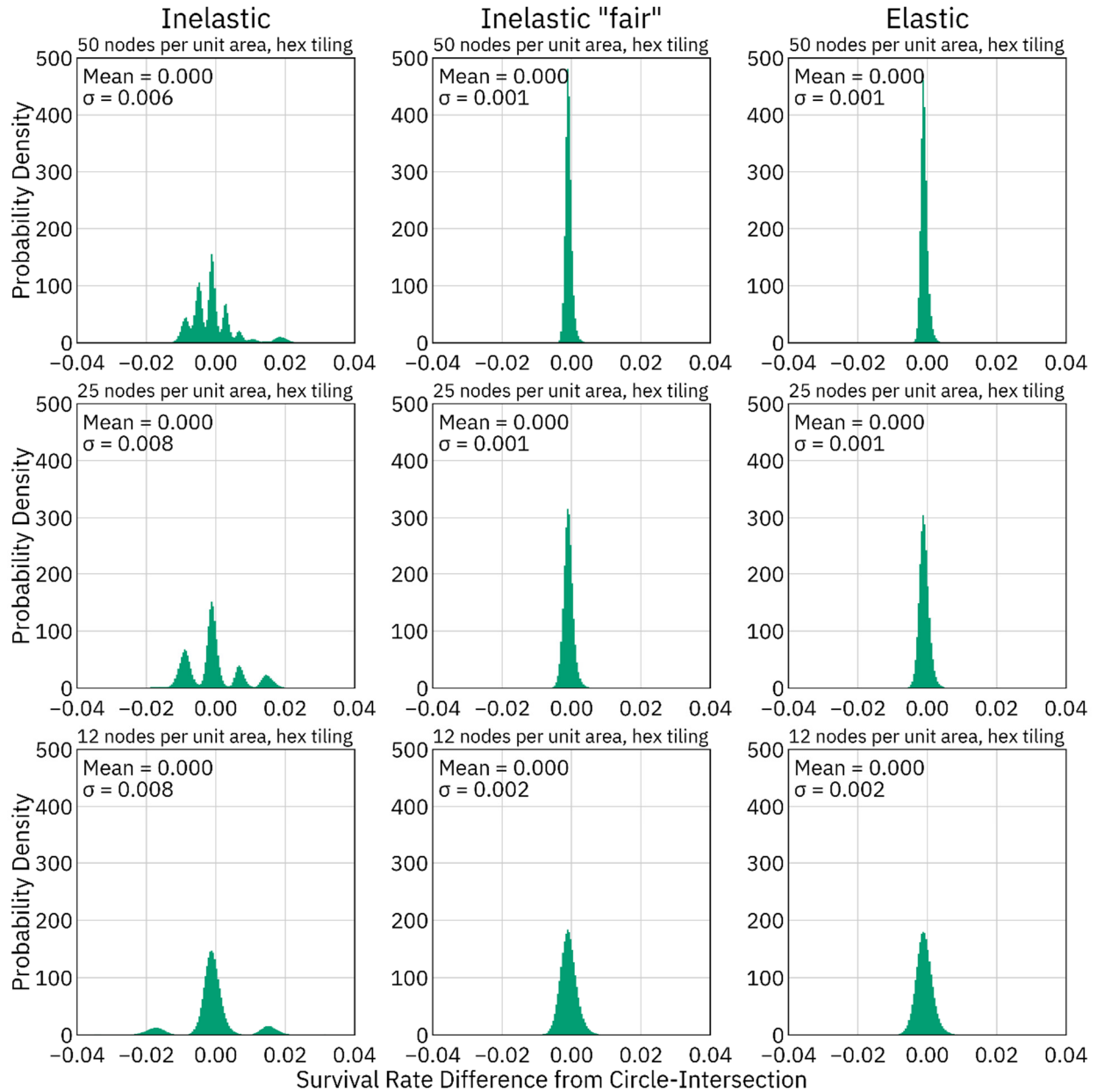
101 We performed an additional assessment of interaction strengths by
102 measuring an “interaction field” between a focal individual and a dense grid of
103 points within interaction range. This analysis was performed with a focal
104 individual placed at a coordinate that minimized the variance between the
105 resource-explicit model and the circle-intersection function, and again at a
106 coordinate that maximized the variance. This analysis was conducted with a
107 hexagonally tiled landscape as well as a square-tiled landscape, each at a density of
108 12, 25, and 50 nodes per unit area, each with both the inelastic and elastic method
109 (Supplemental Figs 8-13).



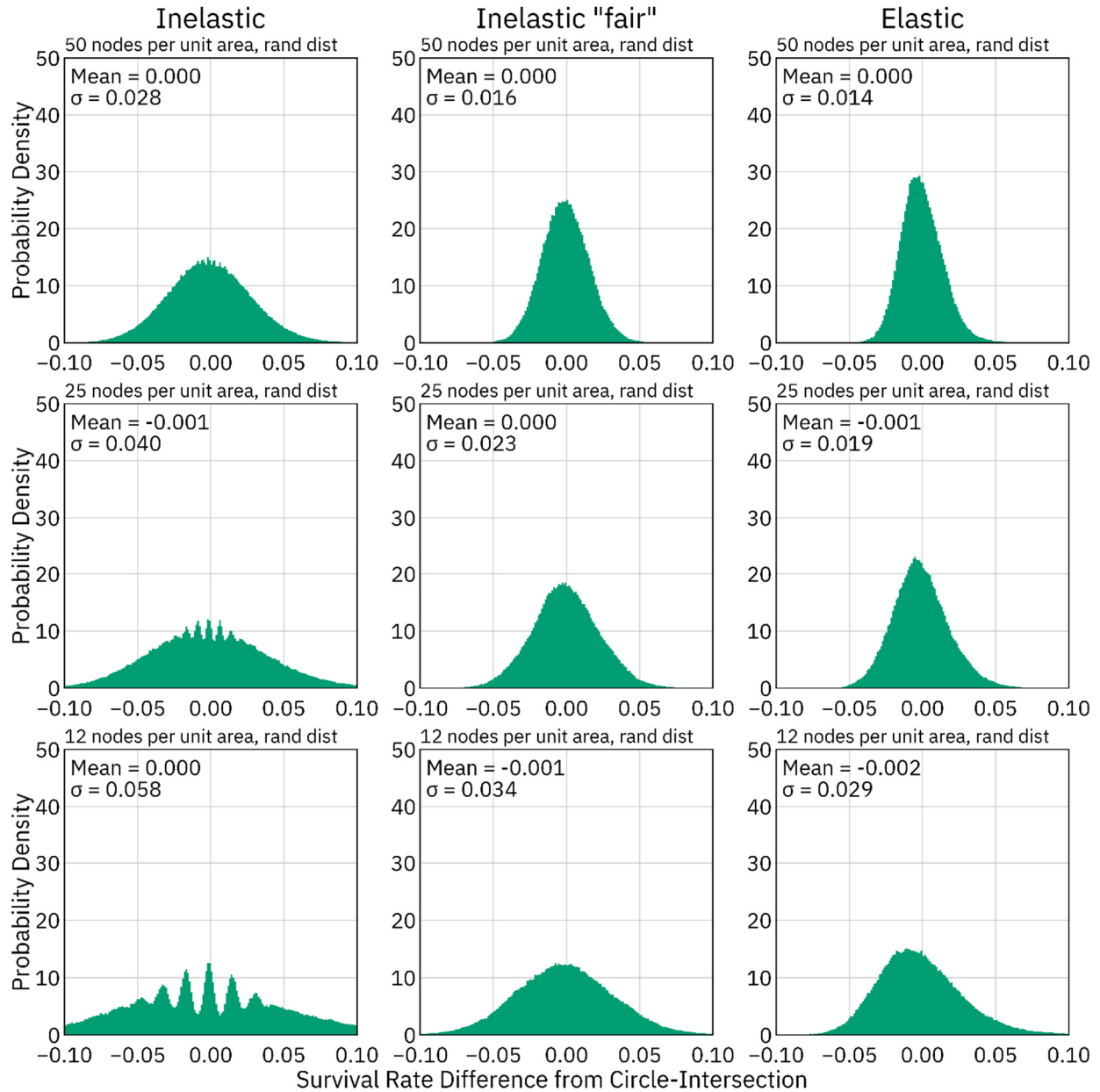
Supplemental Figure 4. Differences in interaction strength between resource-explicit models and the circle-intersection function, hexagonally-tiled. Two million pairwise interaction strengths between randomly placed individuals as measured by the circle-intersection function were subtracted from those measured in resource-explicit models to yield a distribution of the deviation from the circle-intersection function for each model. As node density increases, the standard deviation decreases. These distributions all have a distinctive peak just below 0 due to cases where pairs of individuals have a very small but non-zero interaction strength when using the circle-intersection function, but the small overlapping portion of their foraging areas does not include any resource nodes.



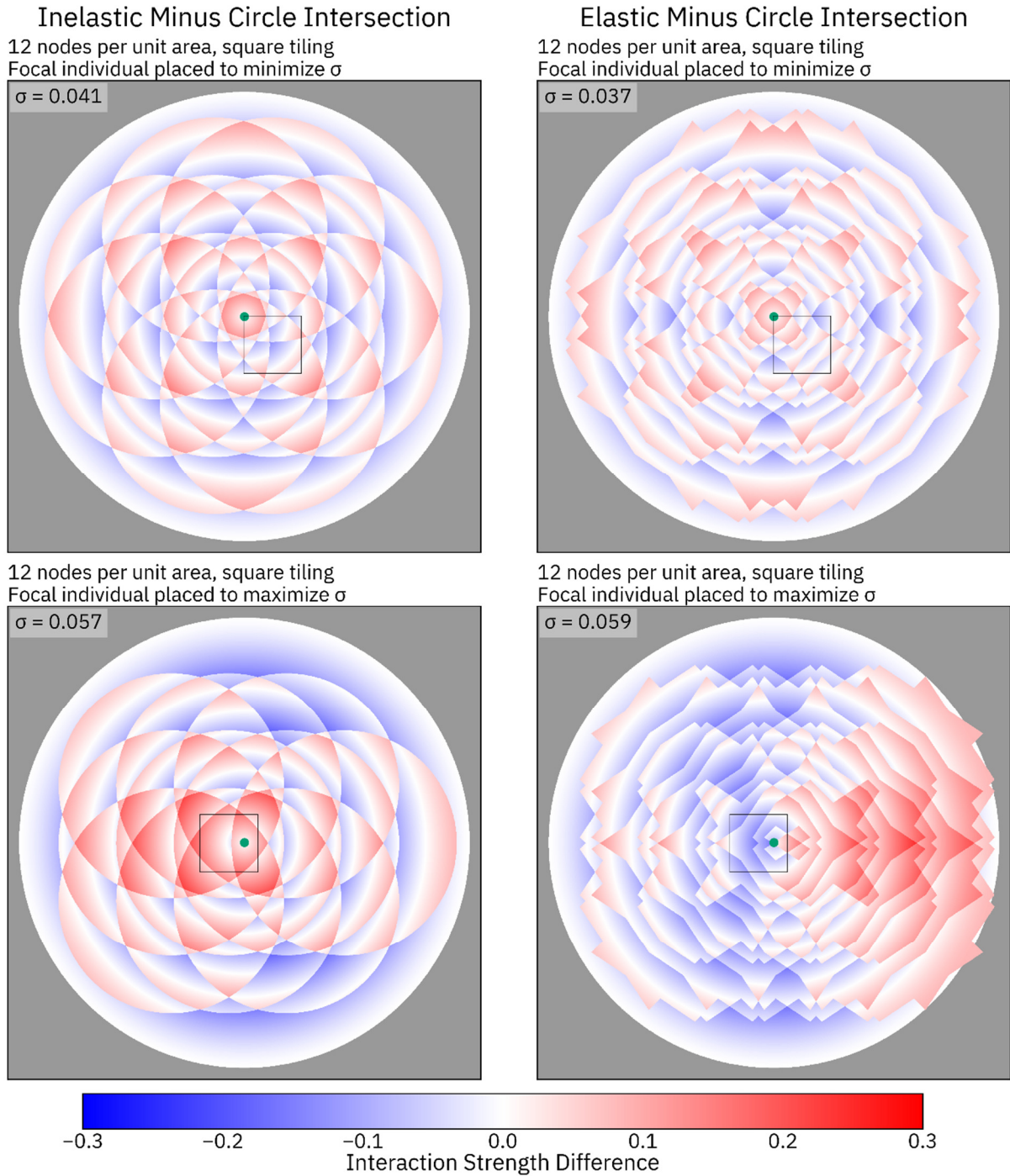
Supplemental Figure 5. Differences in interaction strength between resource-explicit models and the circle-intersection function, random node placement. Two million pairwise interaction strengths between randomly placed individuals as measured by the circle-intersection function were subtracted from those measured in resource-explicit models to yield a distribution of the deviation from the circle-intersection function for each model. As node density increases, the standard deviation decreases. These distributions all have a distinctive peak just below 0 due to cases where pairs of individuals have a very small but non-zero interaction strength when using the circle-intersection function, but the small overlapping portion of their foraging areas does not include any resource nodes. The distinctive peaks at positive values in the elastic model represent cases where the foraging circles do not intersect at all, but two individuals nonetheless share one or two nodes due to a lack of resource nodes closer to the individuals.



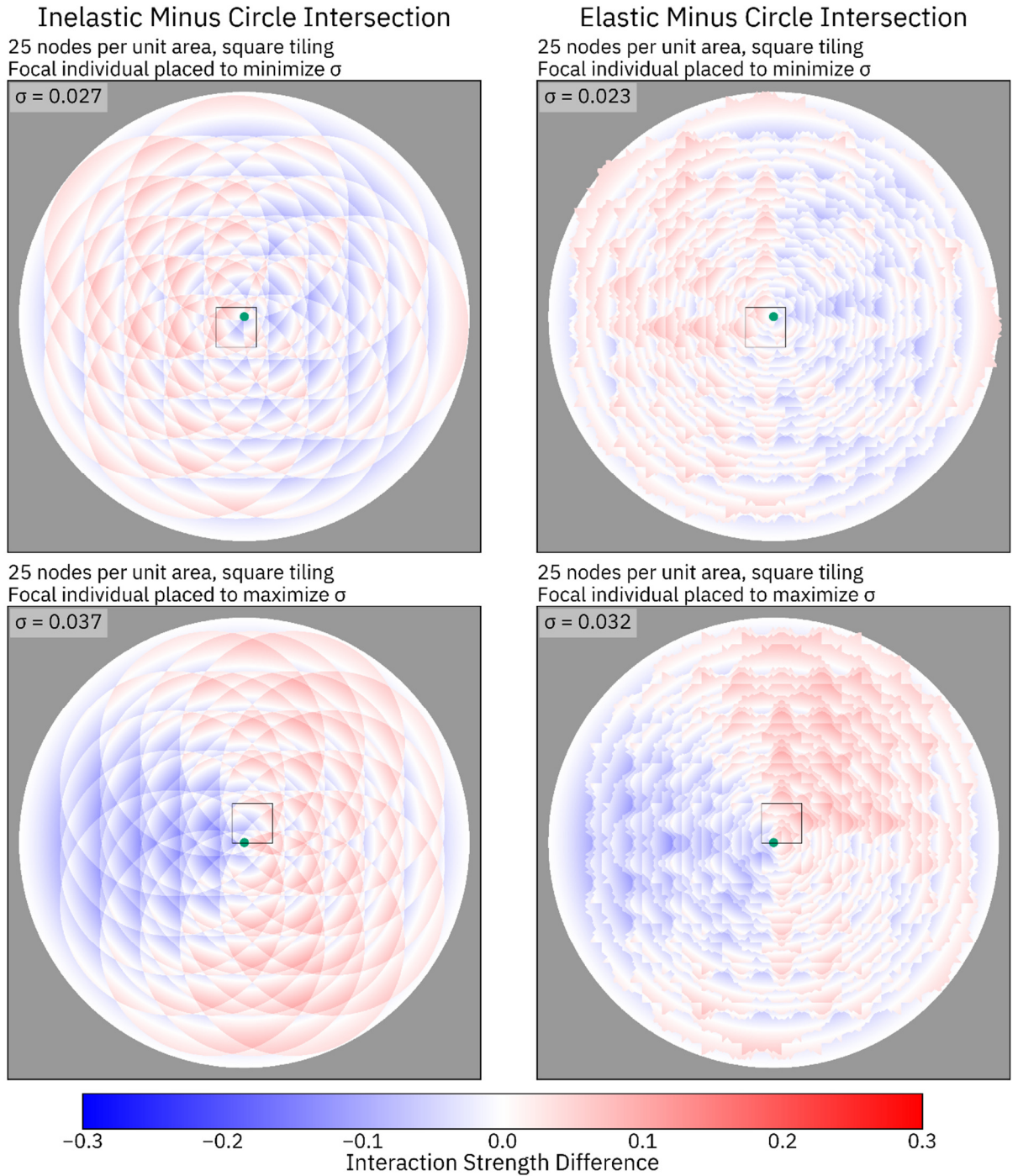
Supplemental Figure 6. Differences in survival rate between resource-explicit models and a direct-interaction model using the circle-intersection function, hexagonally-tiled. The survival rates of 100,000 individuals were measured using the inelastic method, the “fair” inelastic method, the elastic method, and the circle-intersection function. Strengths measured by the circle-intersection function were subtracted from measurements made using the other resource-explicit methods for each individual to yield distributions of differences.



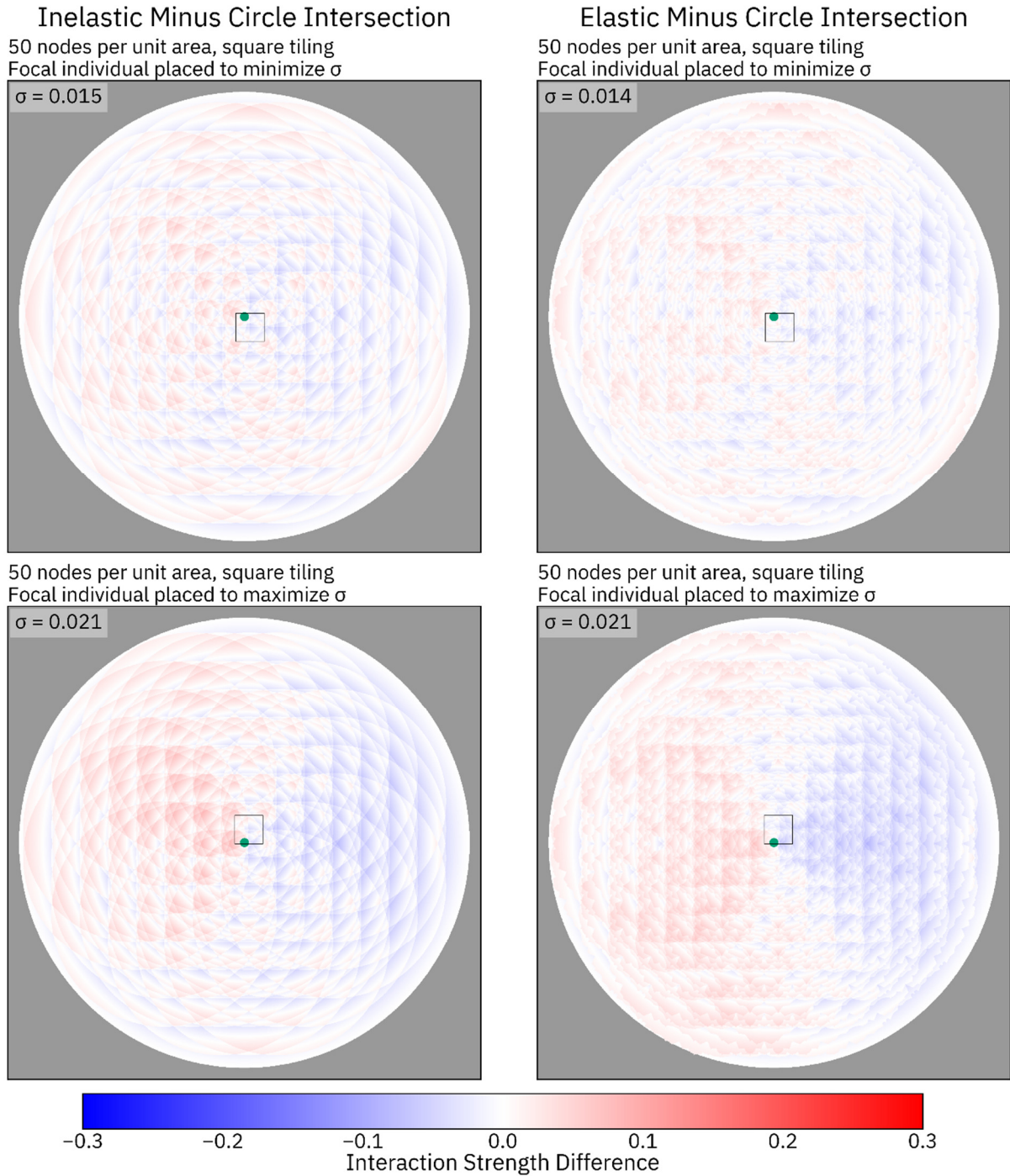
Supplemental Figure 7. Differences in survival rate between resource-explicit models and a direct-interaction model using the circle-intersection function, random node placement. The survival rates of 100,000 individuals were measured using the inelastic method, the “fair” inelastic method, the elastic method, and the circle-intersection function. Strengths measured by the circle-intersection function were subtracted from measurements made using the other resource-explicit methods for each individual to yield distributions of differences.



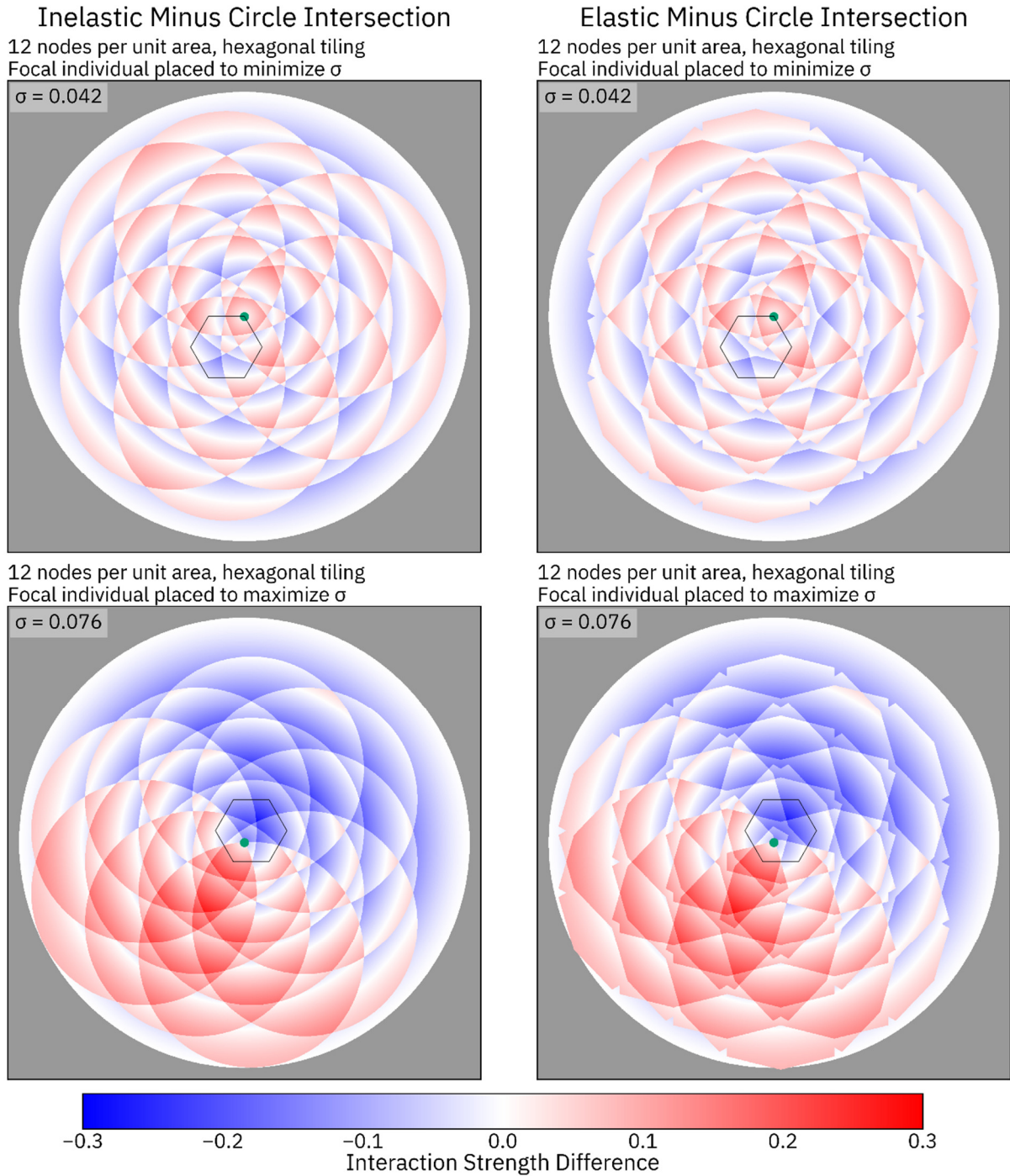
Supplemental Figure 8. Visualization of the resource-explicit interaction, square tiling, 12 nodes per unit area. A central individual (green dot) was placed to either minimize (top panels) or maximize (bottom panels) the standard deviation between the resource-explicit functions and the circle-intersection function. Interaction strength between the central individual and each other pixel of the image was measured using both a resource-explicit method and the circle-intersection function, and the difference is depicted. Blue shading indicates that the circle-intersection function is stronger, while red shading indicates that the resource-explicit interaction is stronger.



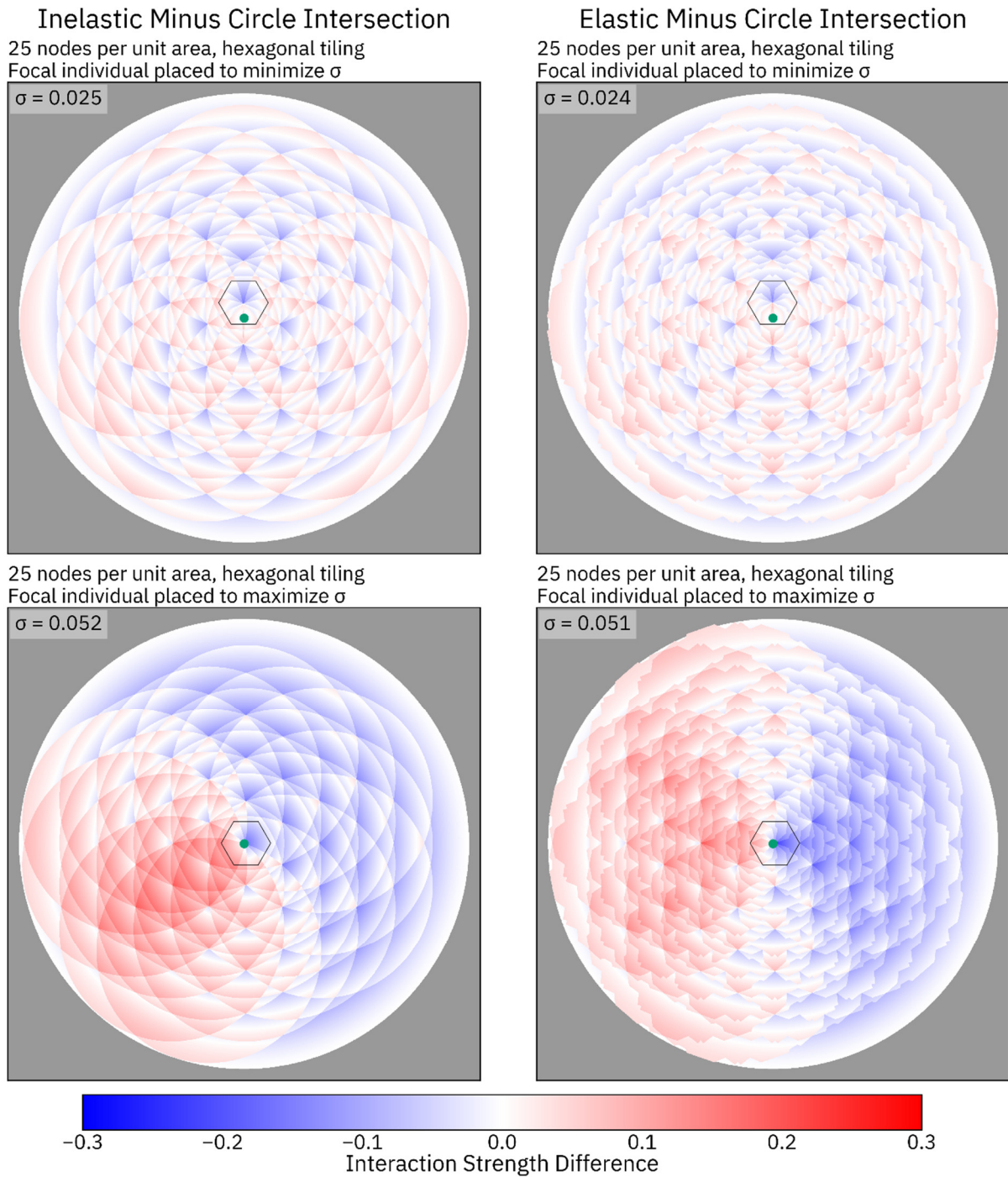
Supplemental Figure 9. Visualization of the resource-explicit interaction, square tiling, 25 nodes per unit area. A central individual (green dot) was placed to either minimize (top panels) or maximize (bottom panels) the standard deviation between the resource-explicit functions and the circle-intersection function. Interaction strength between the central individual and each other pixel of the image was measured using both a resource-explicit method and the circle-intersection function, and the difference is depicted. Blue shading indicates that the circle-intersection function is stronger, while red shading indicates that the resource-explicit interaction is stronger.



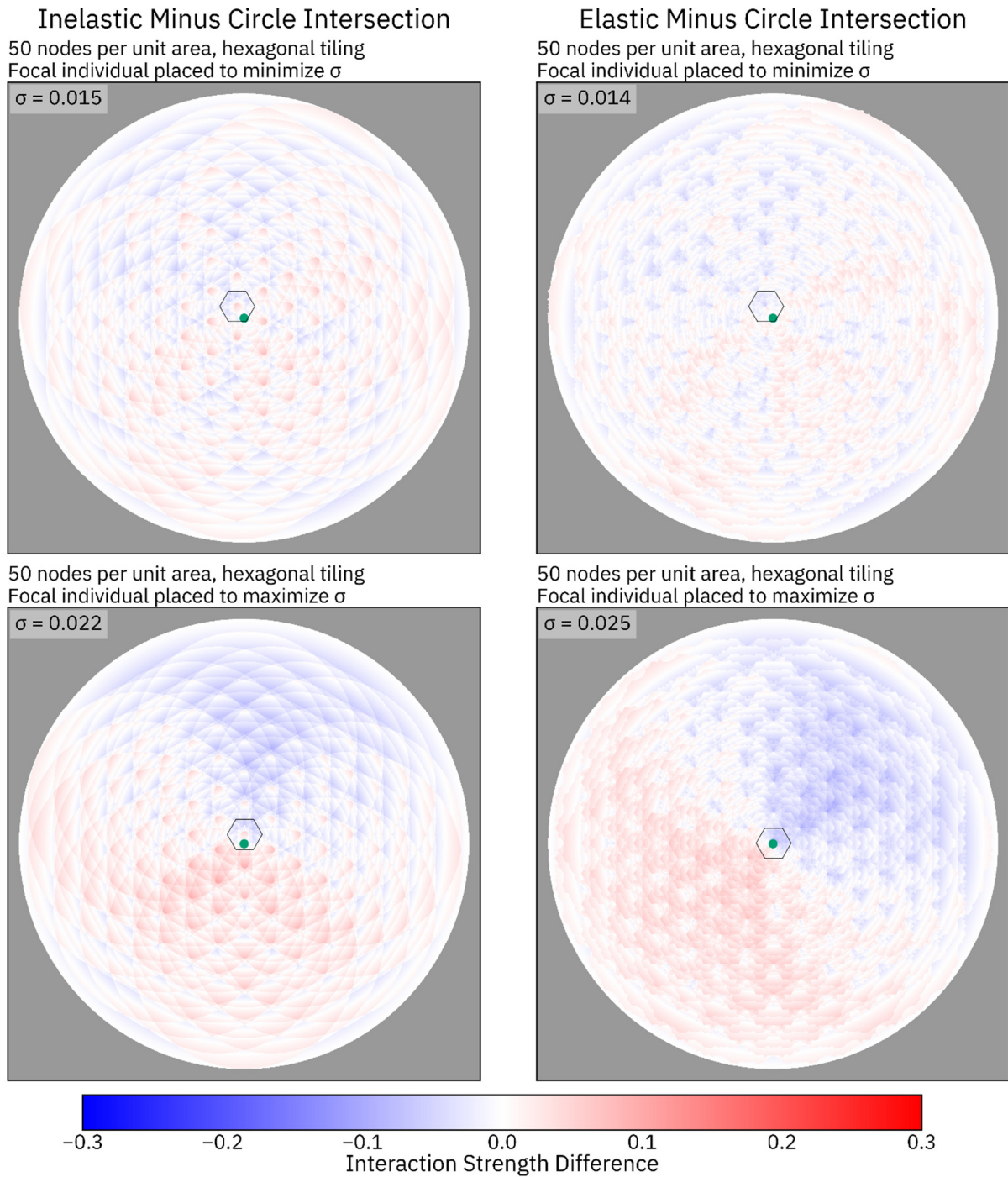
Supplemental Figure 10. Visualization of the resource-explicit interaction, square tiling, 50 nodes per unit area. A central individual (green dot) was placed to either minimize (top panels) or maximize (bottom panels) the standard deviation between the resource-explicit functions and the circle-intersection function. Interaction strength between the central individual and each other pixel of the image was measured using both a resource-explicit method and the circle-intersection function, and the difference is depicted. Blue shading indicates that the circle-intersection function is stronger, while red shading indicates that the resource-explicit interaction is stronger.



Supplemental Figure 11. Visualization of the resource-explicit interaction, hexagonal tiling, 12 nodes per unit area. A central individual (green dot) was placed to either minimize (top panels) or maximize (bottom panels) the standard deviation between the resource-explicit functions and the circle-intersection function. Interaction strength between the central individual and each other pixel of the image was measured using both a resource-explicit method and the circle-intersection function, and the difference is depicted. Blue shading indicates that the circle-intersection function is stronger, while red shading indicates that the resource-explicit interaction is stronger.

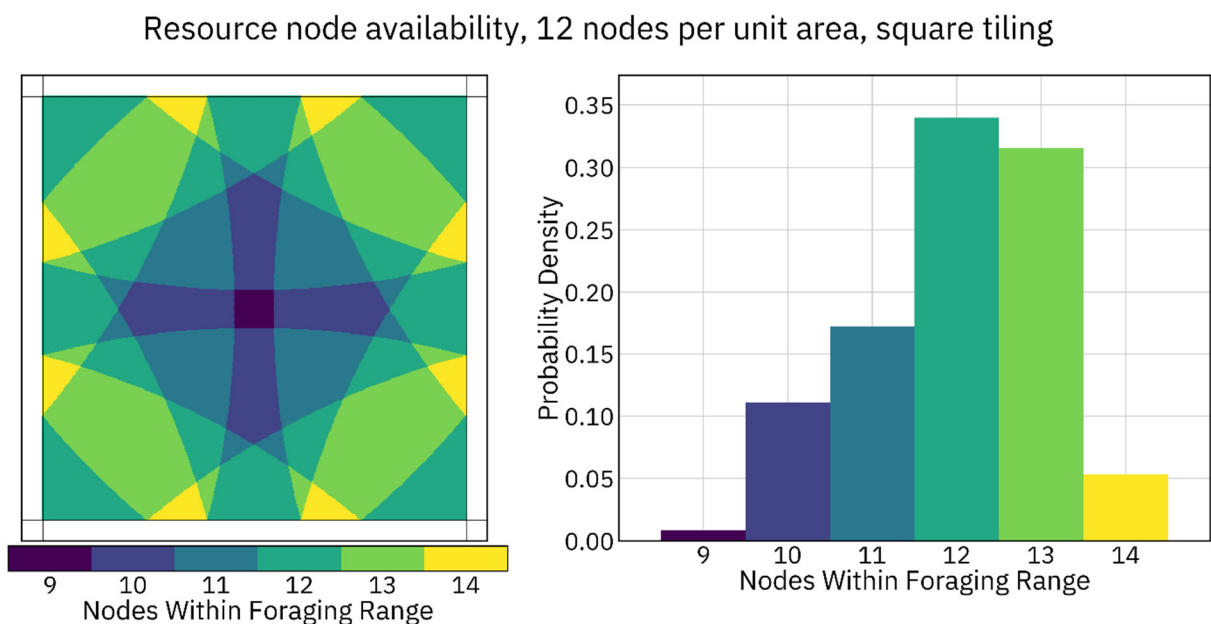


Supplemental Figure 12. Visualization of the resource-explicit interaction, hexagonal tiling, 25 nodes per unit area. A central individual (green dot) was placed to either minimize (top panels) or maximize (bottom panels) the standard deviation between the resource-explicit functions and the circle-intersection function. Interaction strength between the central individual and each other pixel of the image was measured using both a resource-explicit method and the circle-intersection function, and the difference is depicted. Blue shading indicates that the circle-intersection function is stronger, while red shading indicates that the resource-explicit interaction is stronger.



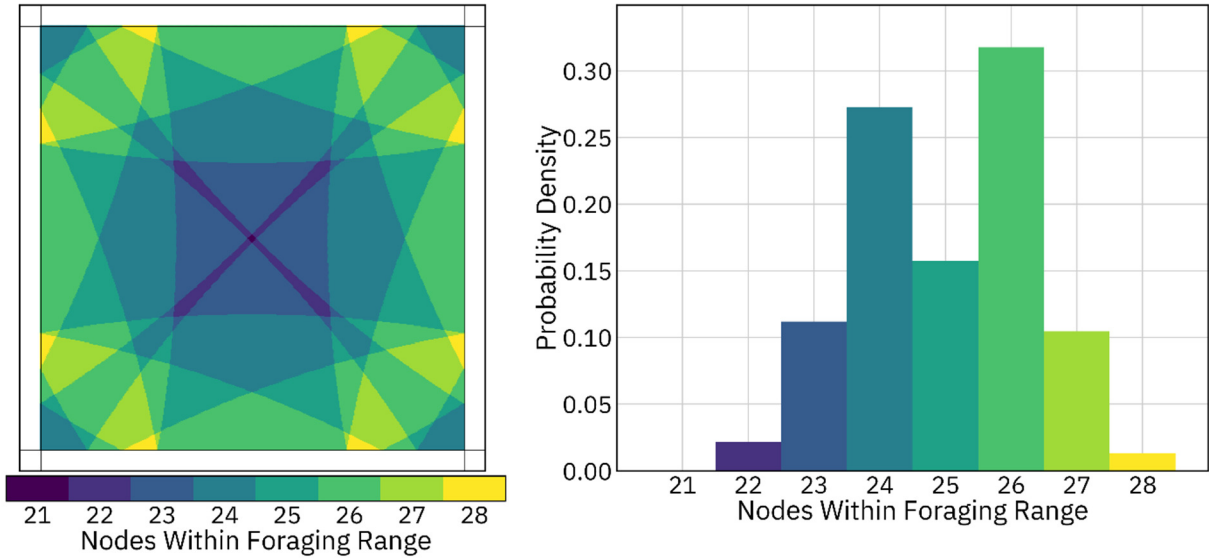
Supplemental Figure 13. Visualization of the resource-explicit interaction, hexagonal tiling, 50 nodes per unit area. A central individual (green dot) was placed to either minimize (top panels) or maximize (bottom panels) the standard deviation between the resource-explicit functions and the circle-intersection function. Interaction strength between the central individual and each other pixel of the image was measured using both a resource-explicit method and the circle-intersection function, and the difference is depicted by blue and red shading. Unlike in Supplemental Figs 8-12, the coordinate that maximized σ differs between the elastic and inelastic method in this case.

110 **Unequal Resource Availability in the Inelastic Model.** In the inelastic
111 implementation of the method, individuals are not guaranteed to forage from the
112 exact nominal foraging area – an individual might forage from more or fewer
113 nodes. When the area is tiled with a uniform grid of nodes, the exact position of an
114 individual relative to this tiling is what determines how many nodes fall within its
115 foraging radius (Supplemental Figs 14-19).



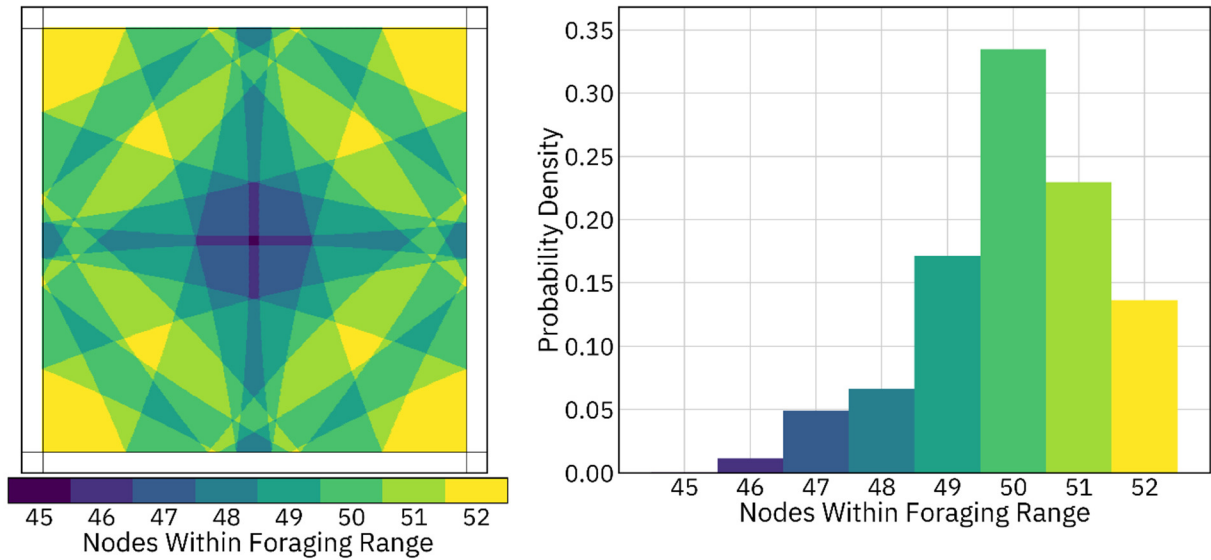
Supplemental Figure 14. Unequal access to resource nodes, square tiling, 12 nodes per unit area. The number of resource nodes within the foraging radius of an individual depends on their location within a square tile. Individuals located in darker regions of the square (left panel) forage from fewer nodes, while those in brighter regions forage from more. The relative area of each color is depicted in the right panel. The mean value of this distribution is 12.00, and the standard deviation is 1.11 (equivalent to 9.2 percent of the foraging area).

Resource node availability, 25 nodes per unit area, square tiling



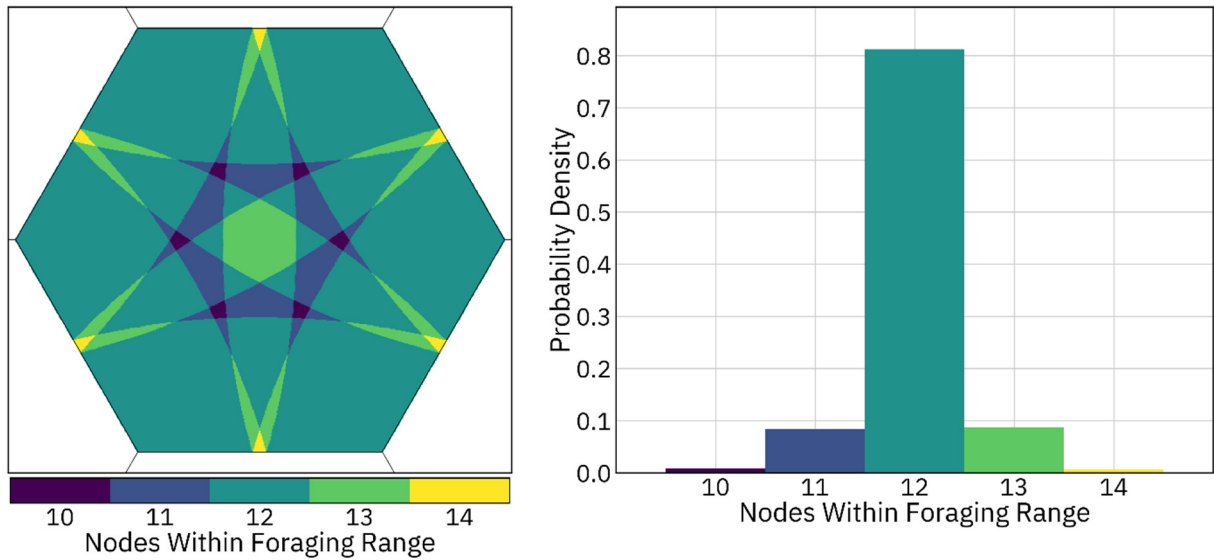
Supplemental Figure 15. Unequal access to resource nodes, square tiling, 25 nodes per unit area. The number of resource nodes within the foraging radius of an individual depends on their location within a square tile. Individuals located in darker regions of the square (left panel) forage from fewer nodes, while those in brighter regions forage from more. The relative area of each color is depicted in the right panel. The mean value of this distribution is 25.00, and the standard deviation is 1.33 (equivalent to 5.3 percent of the foraging area).

Resource node availability, 50 nodes per unit area, square tiling



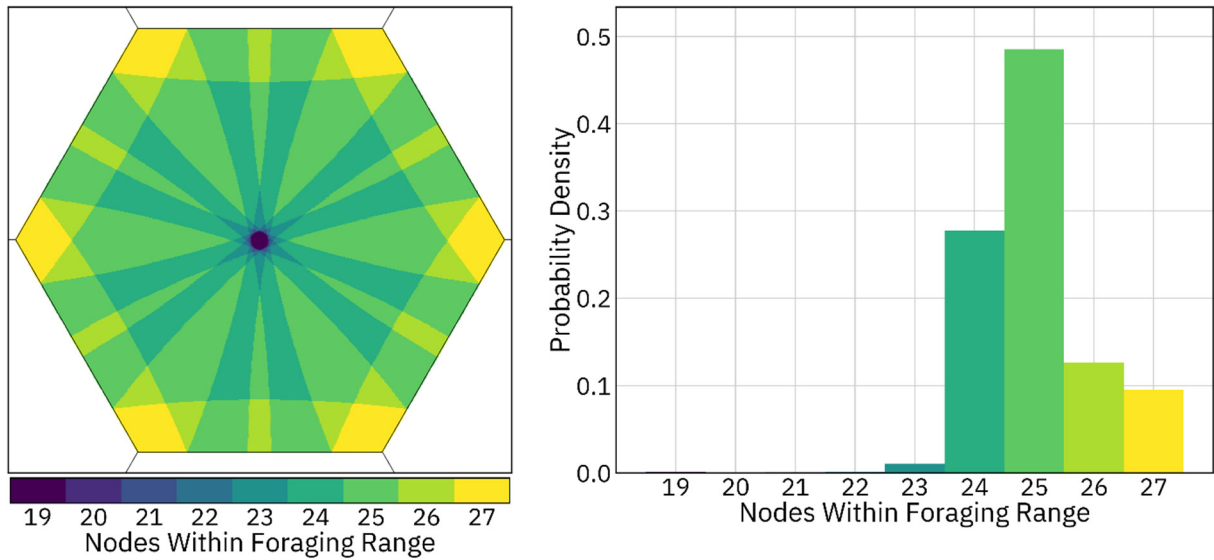
Supplemental Figure 16. Unequal access to resource nodes, square tiling, 50 nodes per unit area. The number of resource nodes within the foraging radius of an individual depends on their location within a square tile. Individuals located in darker regions of the square (left panel) forage from fewer nodes, while those in brighter regions forage from more. The relative area of each color is depicted in the right panel. The mean value of this distribution is 50.00, and the standard deviation is 1.36 (equivalent to 2.7 percent of the foraging area).

Resource node availability, 12 nodes per unit area, hexagonal tiling



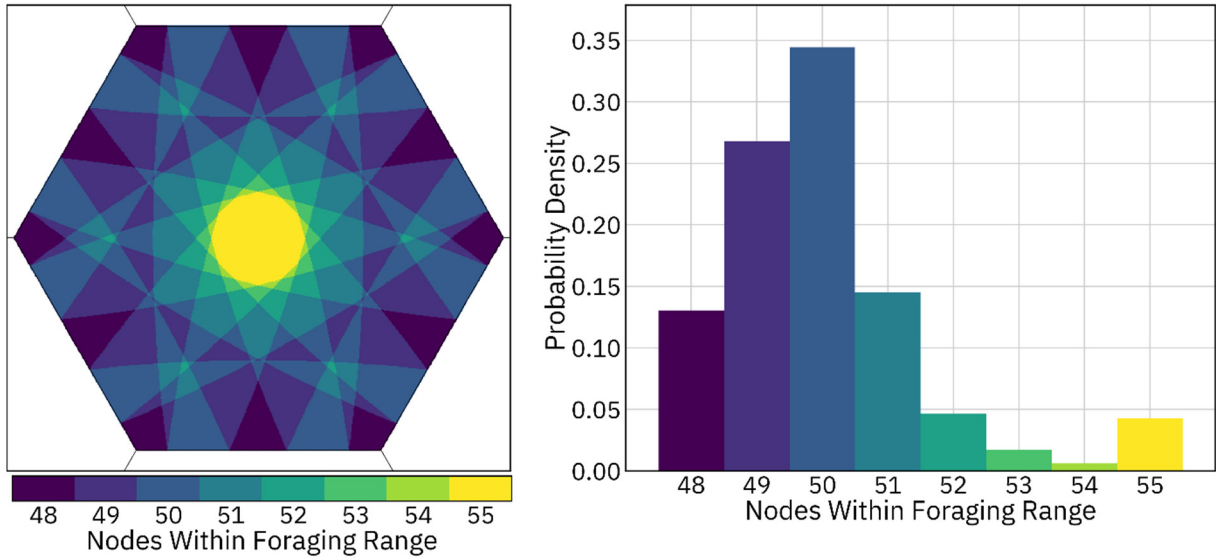
Supplemental Figure 17. Unequal access to resource nodes, hexagonal tiling, 12 nodes per unit area. The number of resource nodes within the foraging radius of an individual depends on their location within a hexagonal tile. Individuals located in darker regions of the hexagon (left panel) forage from fewer nodes, while those in brighter regions forager from more. The relative area of each color is depicted in the right panel. The mean value of this distribution is 12.00, and the standard deviation is 0.48 (equivalent to a 4.0 percent of the foraging area).

Resource node availability, 25 nodes per unit area, hexagonal tiling



Supplemental Figure 18. Unequal access to resource nodes, hexagonal tiling, 25 nodes per unit area. The number of resource nodes within the foraging radius of an individual depends on their location within a hexagonal tile. Individuals located in darker regions of the hexagon (left panel) forage from fewer nodes, while those in brighter regions forager from more. The relative area of each color is depicted in the right panel. The mean value of this distribution is 25.00, and the standard deviation is 0.96 (equivalent to a 3.8 percent of the foraging area).

Resource node availability, 50 nodes per unit area, hexagonal tiling



Supplemental Figure 19. Unequal access to resource nodes, hexagonal tiling, 50 nodes per unit area. The number of resource nodes within the foraging radius of an individual depends on their location within a hexagonal tile. Individuals located in darker regions of the hexagon (left panel) forage from fewer nodes, while those in brighter regions forage from more. The relative area of each color is depicted in the right panel. The mean value of this distribution is 50.00, and the standard deviation is 1.56 (equivalent to a 3.1 percent of the foraging area).

116 COMPUTATIONAL PERFORMANCE OF THE RESOURCE-EXPLICIT MODELS

117 The runtime differences between the square-tiled models and hexagon-tiled
118 models were negligible, representing at most a small fraction of the runtime of the
119 model (Supplemental Table 1). When resource nodes were randomly distributed
120 during each tick of the model, runtimes were slower (Supplemental Table 2).
121 Unsurprisingly, the models most slowed were those with the most resource nodes,
122 which in some cases took almost twice as long to run as a uniformly tiled model
123 with the same population size and node density.

| Model | Node density | Low density (20 individuals per unit area) | | High density (200 individuals per unit area) | |
|--|--------------|--|--|--|--|
| | | 100k individuals Runtime per tick (s) | 1m individuals Runtime per tick (s) | 100k individuals Runtime per tick (s) | 1m individuals Runtime per tick (s) |
| Panmictic | NA | 0.16 | 1.59 | 0.16 | 1.59 |
| Fixed-strength | NA | 3.03 | 38.98 | 17.01 | 233.43 |
| Linear | NA | 3.58 | 45.06 | 23.48 | 302.95 |
| Gaussian | NA | 5.76 | 67.88 | 44.81 | 523.23 |
| Inelastic | 12 | 0.83 | 9.42 | 1.18 | 15.71 |
| | 25 | 0.98 | 11.31 | 1.33 | 17.53 |
| | 50 | 1.33 | 15.05 | 1.57 | 21.27 |
| Inelastic "fair" | 12 | 1.00 | 11.77 | 1.35 | 18.16 |
| | 25 | 1.33 | 15.81 | 1.66 | 22.75 |
| | 50 | 2.04 | 23.50 | 2.26 | 31.15 |
| Inelastic "resource-explicit reproduction" | 12 | 0.98 | 10.95 | 0.82 | 10.59 |
| | 25 | 1.38 | 15.71 | 1.18 | 15.20 |
| | 50 | 2.14 | 24.40 | 1.91 | 24.10 |
| Elastic | 12 | 2.42 | 27.97 | 2.66 | 30.77 |
| | 25 | 3.51 | 40.95 | 3.63 | 41.42 |
| | 50 | 5.85 | 66.10 | 5.59 | 65.45 |

Supplemental Table 1. Model runtimes, hexagonal tiling. Forty measurements of elapsed runtime per tick were collected and averaged for each method at each density and population size and at each of three node-placement densities. For the resource-explicit models depicted in this table, a hexagonal tiling of nodes was used. Color bars show the runtime of each model, on a different scale within each column, relative to the slowest runtime within that column.

| Model | Node density | Low density (20 individuals per unit area) | | High density (200 individuals per unit area) | |
|--|--------------|--|--|--|--|
| | | 100k individuals Runtime per tick (s) | 1m individuals Runtime per tick (s) | 100k individuals Runtime per tick (s) | 1m individuals Runtime per tick (s) |
| Panmictic | NA | 0.16 | 1.59 | 0.16 | 1.59 |
| Fixed-strength | NA | 3.03 | 38.98 | 17.01 | 233.43 |
| Linear | NA | 3.58 | 45.06 | 23.48 | 302.95 |
| Gaussian | NA | 5.76 | 67.88 | 44.81 | 523.23 |
| Inelastic | 12 | 0.95 | 11.94 | 1.27 | 16.77 |
| | 25 | 1.29 | 17.10 | 1.50 | 20.32 |
| | 50 | 1.97 | 27.03 | 1.92 | 26.57 |
| Inelastic "fair" | 12 | 1.23 | 15.44 | 1.51 | 19.65 |
| | 25 | 1.91 | 24.05 | 2.00 | 26.11 |
| | 50 | 3.23 | 41.09 | 2.98 | 38.72 |
| Inelastic "resource-explicit reproduction" | 12 | 1.19 | 14.67 | 0.92 | 12.40 |
| | 25 | 1.88 | 24.37 | 1.38 | 19.27 |
| | 50 | 3.15 | 44.24 | 2.41 | 32.62 |
| Elastic | 12 | 2.47 | 27.73 | 2.70 | 30.73 |
| | 25 | 3.52 | 41.58 | 3.63 | 42.08 |
| | 50 | 5.92 | 67.22 | 5.56 | 65.61 |

Supplemental Table 2. Model runtimes, random node placement. Forty measurements of elapsed runtime per tick were collected and averaged for each method at each density and population size and at each of three node-placement densities. For the resource-explicit models depicted in this table, nodes were randomly distributed across the landscape during each tick of the model. Color bars show the runtime of each model, on a different scale within each column, relative to the slowest runtime within that column.

124 **ADDITIONAL EXTENSIONS**

125 **I. An Implementation of the Elastic Method Optimized for Infrequent Dispersal**

126 An improvement in runtime can be achieved in the elastic model if each
127 individual only disperses infrequently or only a single time (their initial dispersal
128 from their maternal parent), by finding the nearest resource nodes to an individual
129 only after it disperses, and then caching and reusing this list of nodes during each
130 subsequent tick until the individual disperses again or dies. Individuals disperse
131 only once in all of the models presented in this manuscript, but this optimization
132 was not made in the default elastic model in order to provide an accurate reflection
133 of the runtime that could be expected in a model where individuals move during
134 each tick. This optimization is not relevant in a model with non-overlapping
135 generations or in a model with nodes that are re-randomized each time step, since
136 the cached node lists would never be reused.

137 The degree of runtime improvement that this optimization could yield is
138 highly dependent on the demography of the model. In models with a low per-tick
139 mortality and in which individuals only disperse once, this method could be faster
140 than all of the other resource-explicit methods presented in this manuscript. In the
141 model assessed in this study, the mortality rate was quite high (about 80 percent
142 per tick) due to the large number of offspring produced every tick of the model,

143 and the cached node lists only save time for individuals that survive to the next tick
144 to use that cache. Thus, when modified to include this optimization, the elastic
145 model used in this study only increased in speed by a small amount, and was still
146 much slower than the inelastic model. The full code for this modification is
147 provided on GitHub.

148 **II. A Resource-Explicit Model with a Semi-Fixed Population Size**

149 Many analytical models consider populations to consist of a fixed number of
150 individuals. When extending pre-existing analytical models into an individual-
151 based spatial context, it can be desirable to otherwise match the analytical model
152 as closely as possible by maintaining a fixed population size in the spatial model
153 (recognizing that this is biologically unrealistic). A modification of the resource-
154 explicit modeling technique allows for a population size that is fixed except in the
155 event of extreme disruptions to the population.

156 In implementations described in the Methods section, each node is
157 parameterized with some amount of resources that depends on the density of the
158 modeled species and the density of the resource nodes, and each node distributes
159 its resources evenly to all individuals that forage from it. If, for example, there are
160 50 individuals foraging from a node with 10 resources available, each individual

161 will receive 0.2 resources, contributing a 20 percent probability of survival to each
162 of those individuals.

163 In this variant of the model with a semi-fixed population size, resource
164 nodes are instead parameterized by an integer number of “tickets”. Instead of
165 receiving a floating-point amount of resources, individuals instead have a chance
166 to receive a ticket. After tickets are distributed, only individuals who have received
167 a ticket survive. This results in the landscape maintaining a population of exactly
168 the specified carrying capacity, except in the event of a disturbance in the model
169 that causes reproduction to be insufficient to reach that carrying capacity (such as
170 a simulated intervention against a pest population). Note that the population will
171 also not stay exactly at a defined capacity in a model with a marginal habitat
172 quality or a very low birthrate, in which case reproduction may sometimes produce
173 fewer individuals than mortality removes even when no external factors are
174 present.

175 For each of the four variants of the resource-explicit model presented in this
176 manuscript (elastic, inelastic, inelastic “fair”, and inelastic with “resource-explicit
177 reproduction”), the GitHub file repository for this project also contains an
178 equivalent model that has been modified as described above to maintain a semi-
179 fixed population size. This modification results in a moderate performance

180 reduction in the elastic models, but does not appear to noticeably affect the
181 performance of the inelastic models.

182 For modelers seeking to design spatial models that match analytical models
183 as closely as possible, we anticipate that the “fair” variant of the inelastic model
184 may be the best option. This model is faster than the elastic model, yet it avoids the
185 small-scale spatial artifacts present in the default inelastic model which may be
186 undesirable in this context (see Fig. 4 and Supplemental Figs 14-19).

187 **III. A Spatial Model of the South Island of New Zealand**

188 The resource-explicit method has the potential to scale up to modeling large
189 populations in large heterogeneous habitats while maintaining relatively
190 performant runtimes. As an initial exploration into this possibility, we
191 implemented a model on a landscape map of the South Island of New Zealand.
192 Endemic diversity in New Zealand is threatened by the presence of numerous
193 invasive mammal species, and detailed spatial modeling is the first step in
194 investigating potential population control strategies, such as gene drive, in order to
195 maintain and restore biodiversity (Champer, Oakes, et al., 2021).

196 To produce a heterogeneous landscape map of the island, we constructed a
197 habitat suitability map in which we defined habitat quality as a function of
198 elevation, with optimum habitat at about 300 meters above sea level, with quality

199 decreasing at higher and lower elevations. Each resource node was parameterized
200 with resources according to the local elevation near that node. The total area of the
201 South Island is 150,416 km², but mountainous regions were considered to have no
202 accessible resources (Statistics New Zealand, 2010). The amount of the landscape
203 defined as usable habitat by the generic focal species in the model was 100,636
204 km². The nominal foraging area of the focal species was defined as 0.25 km², and
205 the landscape was populated with nodes using a square tiling at a density of 12
206 nodes per 0.25 km². The total number of resource nodes is 4.8 million. Ticks in the
207 model represent monthly intervals. We included seasonality in the model as a per-
208 tick multiplier to the resource value of each node that follows a sinusoidal function
209 with a maximum of 1 in the summer and 0.5 in the winter. The carrying capacity of
210 the focal species across the entire area is 10 million individuals in the summer,
211 with a maximum density of about 50 individuals per 0.25 km² and an average
212 density of about 25 individuals per 0.25 km² (and half these densities in the
213 winter). Node coordinates and resource values were determined in a pre-
214 processing step that generated a CSV file that was reused by all of the replicates of
215 the simulation.

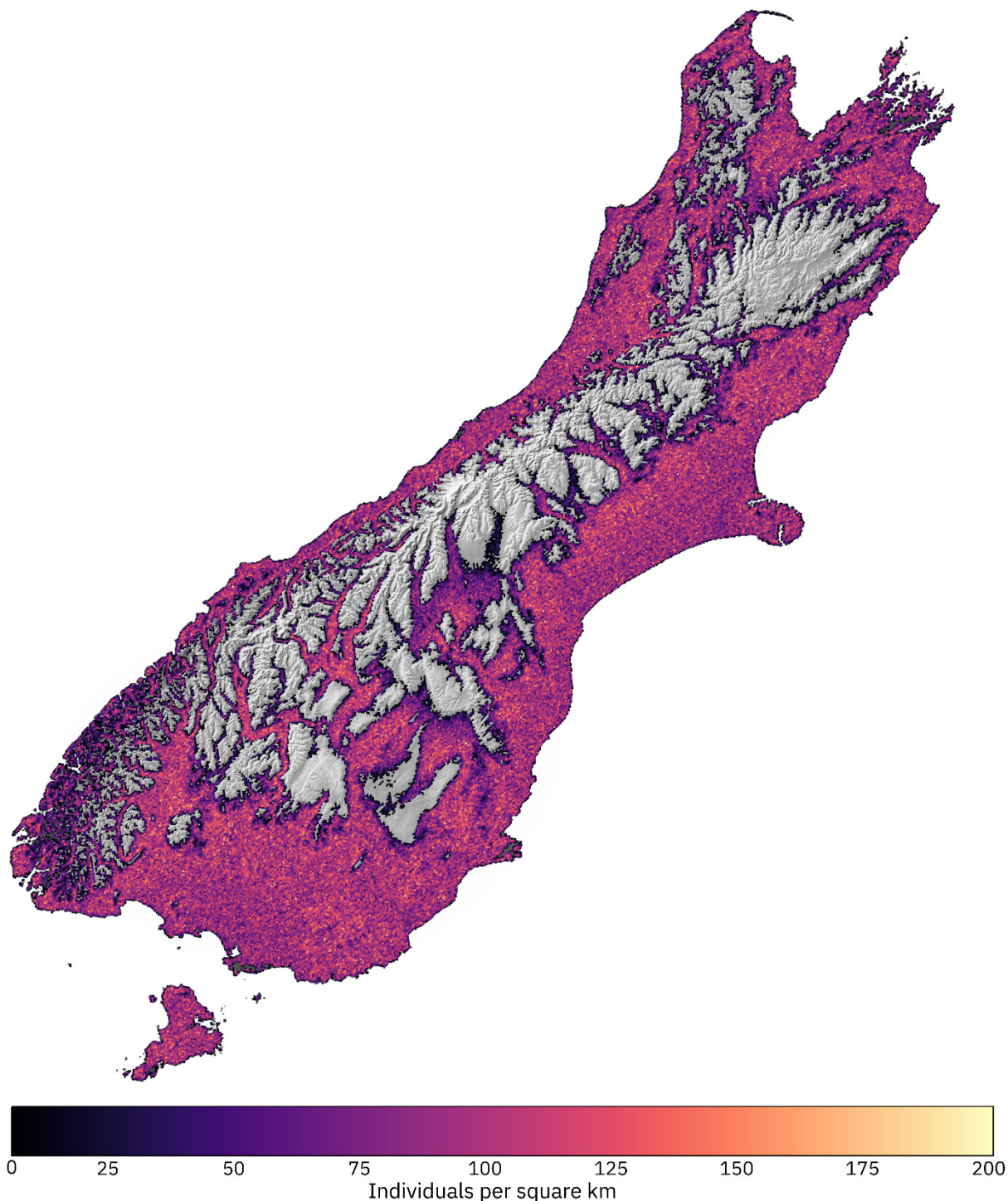
216 The inelastic implementation of the resource-explicit model was chosen for
217 this simulation, in the interest of maximizing the speed of the model. Other than
218 loading node positions from the external CSV file at the outset of the model, the

219 only change to the model was to ensure that individuals were positioned on the
220 landmass at the start of the simulation and were prevented from dispersing into
221 the ocean.

222 No in-depth analyses were conducted of this model, nor were any analogous
223 models constructed for comparison purposes. The average runtime of each tick of
224 this model was under 1.5 minutes even in the summer, when the population was at
225 its maximum size. This is almost certainly sufficiently fast to be used in a study,
226 unless a very large number of ticks needs to be simulated. Though the dynamics
227 within the model were not thoroughly analyzed, a visual assessment indicates that
228 the heterogeneity of the landscape is satisfactorily reflected in the distribution of
229 the population (Supplemental Fig. 20).

230 We also anecdotally observed a number of features of this model that were
231 not explicitly programmed, but which are present as emergent properties of the
232 resource availability of the landscape. These features include landscape
233 fragmentation, with some populations on the landscape (not just the smaller
234 islands) appearing to be completely separated from the main population. We also
235 observed cases of partial fragmentation, wherein some inland populations were
236 separated from a larger coastal population only during the winter, but were once
237 again connected during the summer. We also observed source-sink dynamics in
238 which a population in a marginal habitat area could continue to exist thanks to

239 immigration from higher-quality habitat. This was confirmed by artificially
240 removing individuals from some of the coastal areas of the model, after which
241 some populations further inland collapsed due to marginal habitat quality
242 combined with a lack of immigration from the adjacent (artificially vacated) coastal
243 areas.



Supplemental Figure 20. A heterogeneous landscape model of New Zealand. The modeled area was populated with a square grid of 4.8 million resource nodes and 10 million individuals. Habitat quality was defined as loosely inversely proportional to altitude, with the optimum habitat at about 300 meters above sea level. The color shade gradient denotes the density of individuals. Topographical map image (visible as grayscale shading in areas with no resource nodes) courtesy NASA JPL.